Letters

Controller Design and Implementation of Indirect Current Control Based Utility-Interactive Inverter System

Sunjae Yoon, Hyeongmin Oh, and Sewan Choi

***Abstract*—The utility-interactive inverter with critical load should be able to provide critical loads with a stable and seamless voltage. This letter proposes an indirect current controller which does not include any nonlinear factors in the control block, so that the classical control theory can be applied to the controller design. Also, a phase-locked loop algorithm is proposed to maintain the constant frequency across the critical load during the unintentional islanding since the magnitude is well regulated, but the frequency may vary with the proposed controller. Further, an islanding detection method is proposed for the controller, which does not cause a change in magnitude and frequency of critical load voltage.**

***Index Terms*—Anti-islanding, indirect current control, phase-locked loop (PLL), seamless transfer, utility-interactive inverter.**

I. Introduction

THE utility-interactive inverter with critical loads should operate in stand-alone mode as well as grid-connected mode to provide uninterrupted and continuous power. During the grid-connected mode the inverter is operated to inject power to the grid. In the event of a grid fault, the inverter should detect the islanding and cease to energize the grid by disconnecting the utility-interactive inverter from the grid [1]. During this unintentional islanding, the magnitude, and frequency of the voltage across the critical load may experience severe transient state, since the inverter switch is still closed and the critical load voltage is determined by the amount of injected power and unknown load condition. Further, there exists a large transient across the critical load at turn OFF of the inverter switch if the controller is changed from current controlled mode to voltage controlled mode. Thus, the utility-interactive inverter requires seamless transfer during the unintentional islanding as well as the mode transfer [2].

Several control techniques have been proposed to mitigate large transient associated with mode transfer of the utility-interactive inverter [3]–[6]. However, they did not consider the transient state during the unintentional islanding. The concept of indirect current control method for seamless transfer of the utility interactive inverter was introduced in [7]. An indirect current control of three-phase utility-interactive inverters has been proposed for seamless transfer during whole transition period including both the unintentional islanding and the mode transfer [2].

However, controller design of the indirect current control technique has been on the trial-and-error basis since nonlinear factors, sine and cosine tables, are included in the control block. The frequency of voltage across the critical load may vary in accordance with the amount of injected power and unknown load condition during the unintentional islanding even though the magnitude of the voltage across the critical load is well regulated, which may cause bad effects on the critical load. Further, the conventional islanding detection method based on voltage and frequency variation cannot be applied to this indirect current control, since the voltage across the critical load should always be regulated at the rated values.

In this letter, a modified controller for the indirect current control is proposed to eliminate the sine and cosine tables in the control block, so that the controller design could be based on the classical control theory such as bode diagram and root locus. Also, a phase-locked loop (PLL) technique is proposed to maintain the constant frequency during the unintentional islanding. An active islanding detection method based on harmonic injection which is suitable for indirect current control is also proposed.

II. Proposed Control Algorithm

Fig. 1 shows the circuit diagram of a three-phase utility-interactive inverter with critical load. The proposed indirect current control is to regulate grid-side inductor current i_{Lg} by controlling the magnitude and phase angle of capacitor voltage V_{Cf} so that desired magnitude of grid current which is in phase with the utility voltage is injected to the grid as shown in Fig. 2. From Fig. 2, the nominal value of desired magnitude of *dq*-capacitor voltage can be expressed as

$$V_{Cf,\mathrm{nom}}^{d} = |V_{Lg}| = i_{Lg}^{q*} \times \omega L_g \tag{1}$$

$$V_{Cf,\mathrm{nom}}^{q} = |V_g| \,. \tag{2}$$

Fig. 3 shows the proposed control block diagram for grid-connected and stand-alone operations of the three-phase

Manuscript received March 16, 2012; revised June 12, 2012; accepted July 17, 2012. Date of current version September 11, 2012. Recommended for publication by Associate Editor J. Biela.

S. Yoon is with LSIS R&D Center, LS Industrial Systems Company, Gyeonggi-do 431-080, Korea (e-mail: sjyoona@lsis.biz).

H. Oh is with HAE R&D Lab, LG Electronics Company, Seoul 153-802 Korea (e-mail: hyeongmin.oh@lge.com).

S. Choi is with the Department of Electrical and Information Engineering, Seoul National University of Science and Technology, Seoul 139-743, Korea (e-mail: schoi@seoultech.ac.kr).

Color versions of one or more of the figures in this paper are available online at http://ieeexplore.ieee.org.

Digital Object Identifier 10.1109/TPEL.2012.2210247

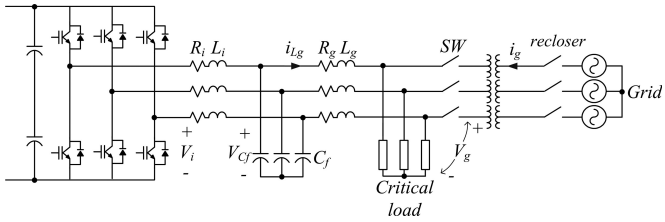

Fig. 1. Circuit diagram of a three-phase utility-interactive inverter.

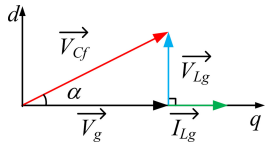

Fig. 2. Phasor diagram illustrating the proposed indirect current control.

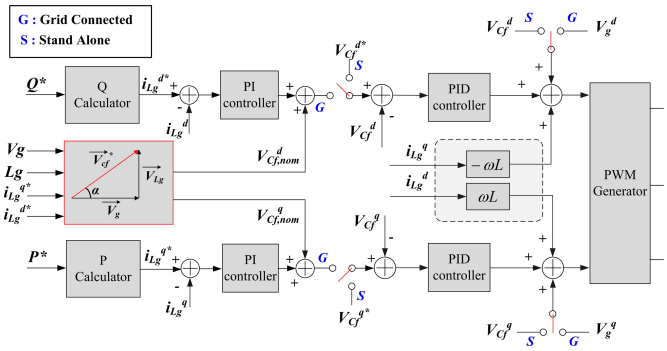

Fig. 3. Block diagram of the proposed indirect current control for a three-phase utility-interactive inverter.

utility-interactive inverter. The controller consists of an outer current control loop for regulating desired amount of injection current and an inner voltage control loop for controlling instantaneous capacitor voltage. A double-loop control with outer current and inner voltage loops is used for the grid-connected mode. A single loop voltage control is used for the stand-alone mode. The *dq*-capacitor voltage reference can be obtained by adding the nominal value of desired magnitude of *dq*-capacitor voltage to the output of the *dq*-grid-side inductor current controller. Assuming that the decoupling is done by controller, the control block diagram shown in Fig. 3 can be simplified as shown in Fig. 4. The whole block diagram in Fig. 4 illustrates grid-connected mode, and the part within shadowed box in Fig. 4 illustrates stand-alone mode. The closed-loop transfer function of the inner voltage loop is obtained by

$$\frac{v_{Cf}^{dq}(s)}{v_{Cf}^{dq*}(s)} = \frac{\left(K_{pv}s + K_{iv} + K_{dv}s^2\right)\left(L_g s + R_g\right)}{As^4 + Bs^3 + Cs^2 + Ds + E} \tag{3}$$

where, $A = L_i C_f L_g$, $B = R_i C_f L_g + L_i C_f R_g + K_{dv} L_g$, $C = K_{dv} R_g + L_i + R_i C_f R_g + K_{pv} L_g + L_g$, $D = K_{pv} R_g + R_i + K_{iv} L_g + R_g$, $E = K_{iv} R_g$

The forth-order system can be approximated by the second-order system as long as the real part of the dominant roots

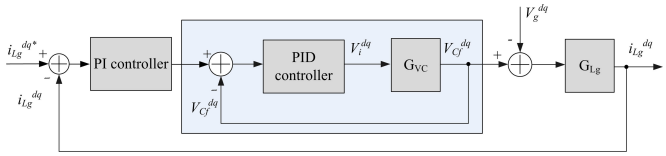

Fig. 4. Simplified block diagram of the proposed indirect current control.

is less than one tenth of the real part of the third and fourth roots [12]. By equating the approximated second-order system to the simple second-order system with desired damping factor ζ_v and natural frequency ω_v, voltage controller gains can be obtained by

$$K_{pv} = \omega_v^2\left(1 + 2\zeta_v^2 m\right) L_i C_f - 1 - \left(L_i / L_g\right) \tag{4}$$

$$K_{iv} = \zeta_v \omega_v^3 m / L_g \tag{5}$$

$$K_{dv} = \zeta_v \omega_v \left(2 + m\right) L_i C_f - R_i C_f \tag{6}$$

where, in general, m is chosen to be greater than 10.

Assuming that the control bandwidth of inner voltage loop is larger than that of the outer current loop, the transfer function of the inner voltage loop can be approximated to one. Then the closed-loop transfer function of the whole system becomes

$$\frac{i_{Lg}^{dq}}{i_{Lg}^{dq*}} = \frac{K_{pi}s + K_{ii}}{s^2 L_g + \left(R_g + K_{pi}\right)s + K_{ii}}. \tag{7}$$

In the same way, from characteristic (7), given desired damping factor ζ_i and natural frequency ω_i of the output current loop, current controller gains can be obtained by

$$K_{pi} = 2\zeta_i \omega_i L_g - R_g \tag{8}$$

$$K_{ii} = \omega_i^2 L_g. \tag{9}$$

For an example, calculation of controller design the *LCL* filter values of $L_i = 1.78$ mH, $C_f = 3$ uF, $L_g = 3$ mH are obtained by [2] assuming $P_o = 1$ kW, $V_g = 110$ V, $R_i = 10$ mΩ, $R_g = 20$ mΩ.

If the desired damping and controller bandwidth of the inner voltage loop are 0.7 and 20 000 rad/s, respectively, the bode diagram of the voltage loop gain can be obtained by using (4)–(6), as shown in Fig. 5(a). It can be seen that the phase margin and cutoff frequency of the voltage loop are around 75° and 20 900 rad/s which are close to the desired values. Also, if the desired damping and controller bandwidth of the outer current loop are 0.6 and 500 rad/s, respectively, the bode diagram of the current loop gain can be obtained by using (8) and (9), as shown in Fig. 5(b). It can be seen that the phase margin and cutoff frequency of the voltage loop are around 67.6° and 534 rad/s.

III. Proposed PLL Algorithm

Even though the proposed indirect current control is able to provide well regulated voltage across the critical load, constant frequency cannot be guaranteed with the conventional PLL algorithm, since the frequency of the inverter output voltage is adjusted such that the phase of the inverter output voltage is synchronized to the grid voltage, as shown Fig. 6(a) [9], [10].

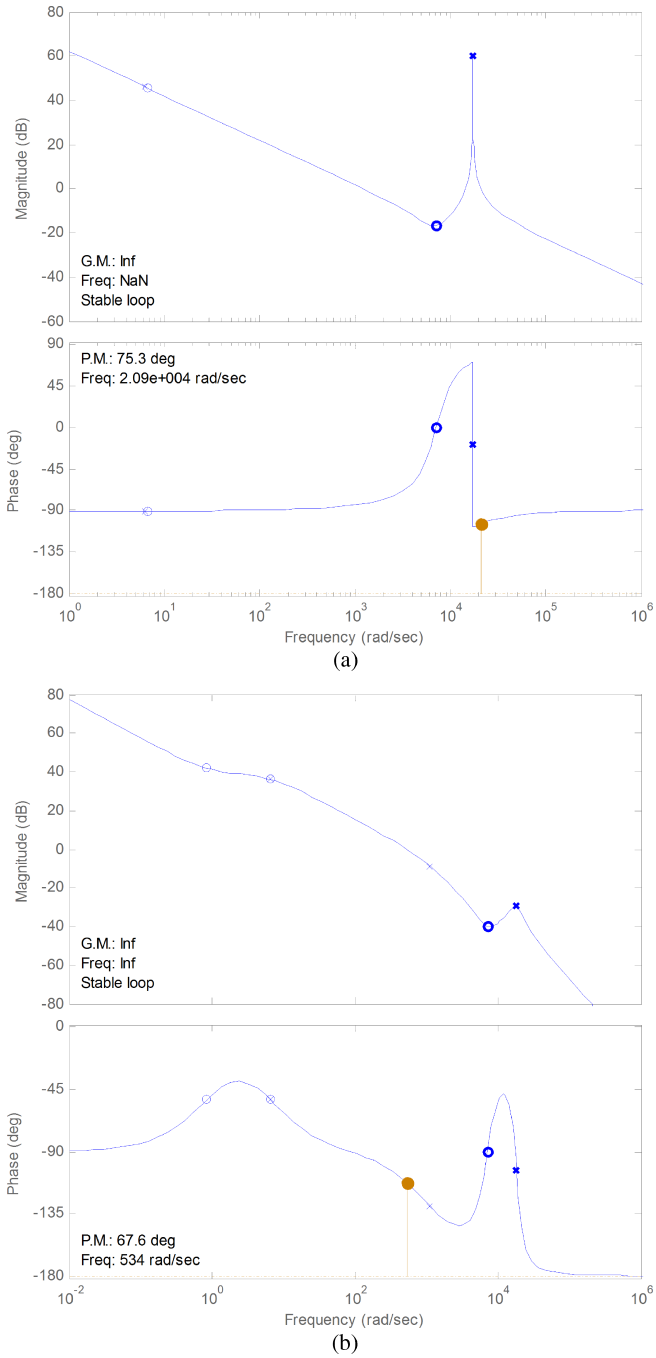

Fig. 5. Bode diagram (a) inner voltage control-loop gain and (b) outer current control-loop gain.

Therefore, when an islanding occurs the frequency of the critical load voltage may change according to magnitude difference between inverter output power and demanded critical load power. This leads to frequency deviation of the critical load voltage and the phase angle always ranges from $-\pi$ to π since the frequency of the inverter output voltage is adjusted such that the inverter output voltage is synchronized to the grid voltage, as shown in Fig. 7(a), which may cause bad effects on the critical load.

Fig. 6(b) shows the block diagram of the proposed PLL algorithm. The reference phase angle θ is obtained by summation of

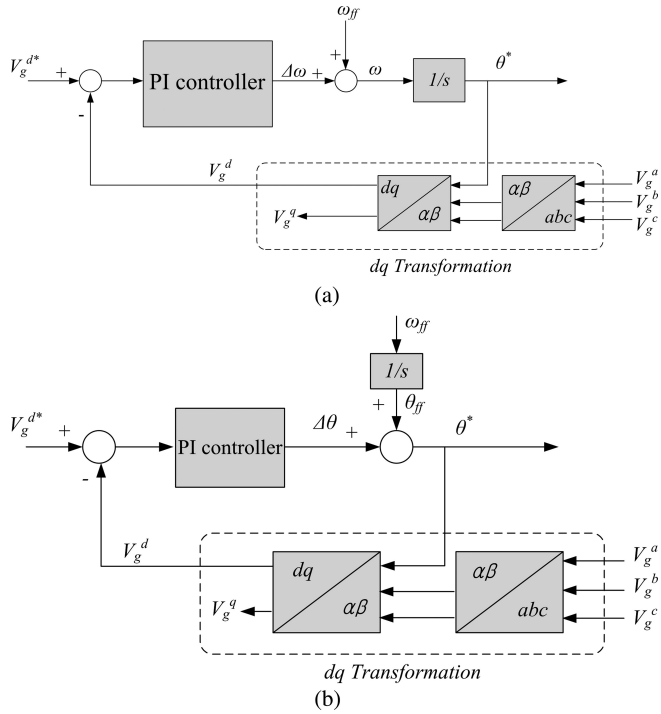

Fig. 6. *dq*-PLL algorithm: (a) conventional and (b) proposed.

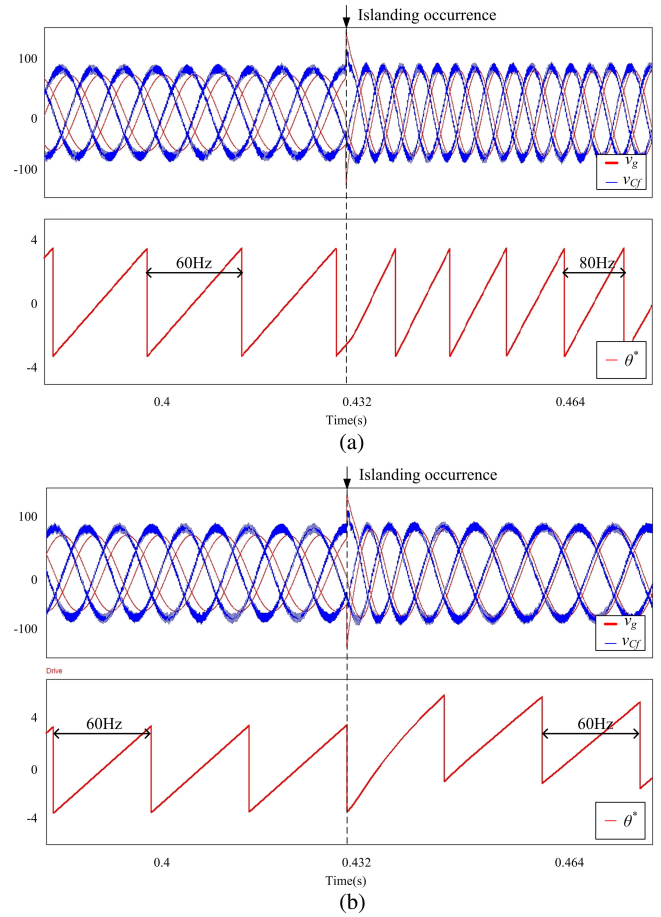

Fig. 7. Simulation of the PLL algorithm when the islanding occurs (a) conventional and (b) proposed.

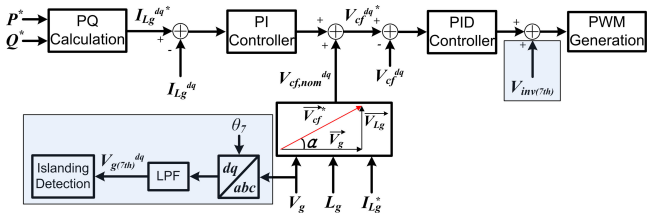

Fig. 8. Control block diagram including the proposed anti-islanding method.

feedforward angle $\theta_{\rm ff}$ which is integral of rated frequency of the grid voltage and compensating angle $\Delta\theta$ which is the output of the PI controller for d-axis grid voltage. Since the slope of the reference phase angle θ is constant, the output frequency of the PLL maintains at $\omega_{\rm ff}$ without regard to the compensating angle $\Delta\theta$. Therefore, during the unintentional islanding the controller is capable of providing the critical load with constant frequency as well as constant voltage across the critical load without regard to the load condition and the range of the phase angle is changed during islanding operation, since the phase angle of the inverter output voltage is adjusted such that the inverter output voltage is synchronized to the grid voltage, as shown in Fig. 7(b).

IV. Proposed Anti-Islanding Algorithm

The conventional anti-islanding method generally detects variation in voltage and frequency of the critical load [11], which is determined by differences between real and reactive power consumed by the critical load and real and reactive power supplied by the inverter. However, with the proposed indirect current control and proposed PLL algorithm the voltage and frequency of the critical load do not change when the islanding occurs. Therefore, the conventional islanding detection method based on voltage and frequency variations cannot be applied to the proposed indirect current control. Fig. 8 illustrates the control block diagram including the proposed anti-islanding method. The proposed islanding detection method injects a harmonic component $V_{\rm inv(7th)}$ into output of voltage controller. When the grid is connected, the voltage of the critical load is imposed by the grid, and its waveform is not altered by the injected harmonic component. When an islanding condition occurs, the critical load voltage follows the waveform of the harmonic component injected by the inverter. But the magnitude of the injected harmonic component should be limited, for example, less than 4% of the fundamental component according to IEEE Standard 1547-2003, since the excessive harmonic injection may cause a severe distortion in grid current. The proposed active anti-islanding method detects islanding condition by measuring the harmonic voltage variation as shown in Fig. 9.

Fig. 10 shows a flowchart of the proposed active anti-islanding algorithm for the indirect current control. First, grid voltage V_g is sampled and transformed into the rotating dq-reference frame with the injected harmonic frequency, and then the injected harmonic components are obtained through low-pass filtering of d-axis and q-axis components. As far as actual value $V^q_{g(7\rm th)}$ of q-axis is larger than user defined value $V^{q*}_{g(7\rm th)}$, the index "*count*" keeps increasing. When it becomes the limiting value $\rm count_{max}$

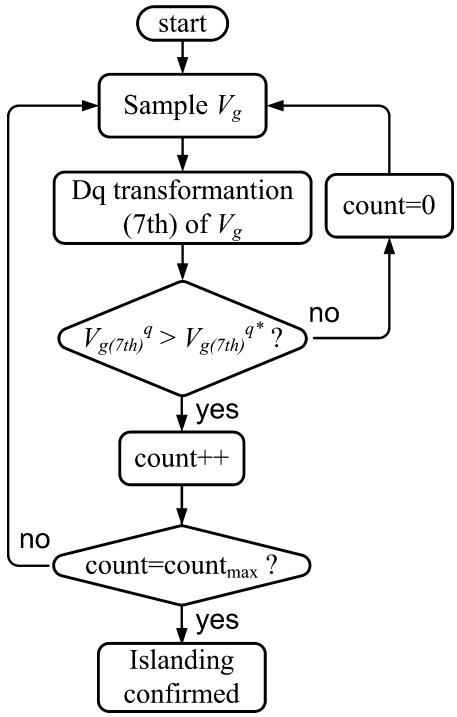

Fig. 9. Flowchart of the proposed anti-islanding algorithm.

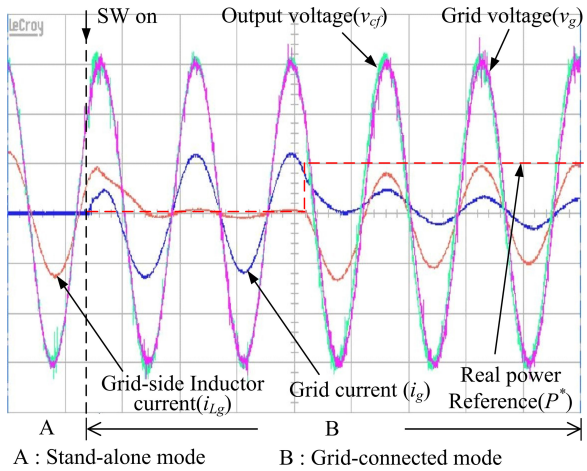

Fig. 10. Experimental waveforms of the proposed control showing the mode transfer from stand-alone mode to grid-connected mode.

the islanding can be confirmed. The user defined value $V^{q*}_{g(7\rm th)}$ should carefully be chosen since smaller user defined values may result in frequent tripping of inverter switch. The limiting value $count_{\rm max}$ should be selected to be smaller than 2 s to meet IEEE Standard. 929-2000 or IEEE Standard 1547-2003.

V. Experimental Results

The system parameters used in the experiment are as follows: output power $P_o = 1$ kW; grid voltage $V_g = 110$ V; line frequency $f = 60$ Hz; switching frequency $f_s = 10$ kHz; $L_i = 1.78$ mH; $C_f = 3$ uF; $L_g = 3$ mH; and $count_{\rm max}$ is 150. Fig. 10 shows experimental waveforms for the transfer from stand-alone mode to grid-connected mode. After the phase match the inverter

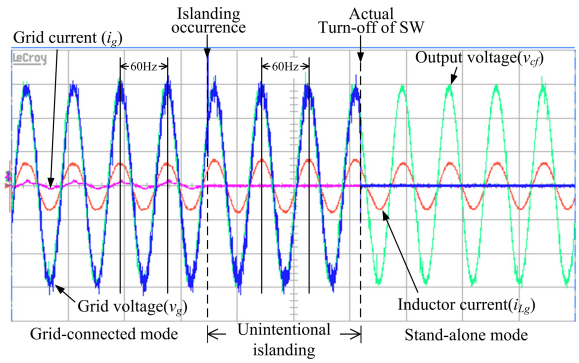

Fig. 11. Experimental waveforms of the proposed control showing the mode transfer from grid-connected mode to stand-alone mode.

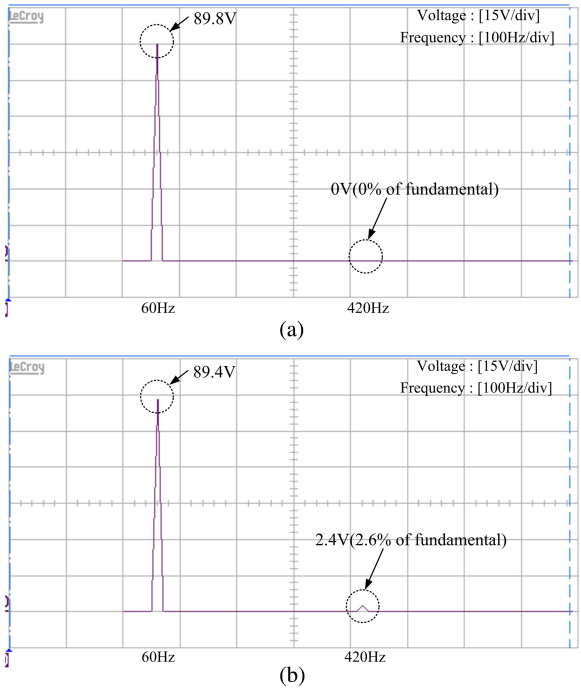

Fig. 12. FFT of critical load voltage: (a) before islanding occurrence and (b) during unintentional islanding.

switch is closed, then the grid-side inductor current reduces to zero since the commanded real and reactive power are zeroes. Then the demanded critical load power is supplied from the grid. With the signal for grid current injection the grid current i_{Lg} is gradually increased according to its commanded real power. Fig. 11 shows experimental waveforms for the transfer from grid-connected mode to stand-alone mode. It should be noted that there is no change in voltage and frequency of the critical load during an unintentional islanding. Any noticeable transient is not observed across the load throughout the whole transition period including both the unintentional islanding and the mode transfer, which is performed right after actual turn off of the inverter switch. Fig. 12 illustrates the validity of the proposed islanding detection method which detects an islanding condition by injecting the seventh harmonic component to the inverter output voltage. Fig. 12(a) shows fast Fourier transform (FFT) of critical load voltage before islanding occurrence. The seventh harmonic component injected for islanding detection does not appear in the critical load voltage, since the voltage of the critical load is imposed by the grid. However, when an islanding condition occurs, the seventh harmonic component is observed in the critical load voltage, as shown in Fig. 12(b).

VI. Conclusion

In this letter, an indirect current controller which does not include any nonlinear factors in the control block has been proposed so that the classical control theory can be applied to the controller design. Also, a PLL algorithm which is able to maintain the constant frequency across the critical load during the unintentional islanding has been proposed. The proposed active islanding detection method based on harmonic injection is suitable for the indirect current controller, which does not cause a change in magnitude and frequency of critical load voltage. The proposed control method has been validated through experiment.

References

[1] *IEEE Standard for Interconnecting Distributed Resources With Electric Power Systems, IEEE Standard 1547*, 2003.
[2] J. Kwon, S. Yoon, and S. Choi, "Indirect current control for seamless transfer of three-phase utility interactive inverters," *IEEE Trans. Power Electron.*, vol. 27, no. 2, pp. 773–781, Feb. 2012.
[3] R. Tirumala, N. Mohan, and C. Henze, "Seamless transfer of grid-connected PWM inverters between utility-interactive and stand-alone modes," in *Proc. IEEE Appl. Power. Electron. Conf. Expo.*, Mar. 2002, pp. 1081–1086.
[4] G. Q. Shen, D. H. Xu, and X. M. Yuan, "A novel seamless transfer control strategy based on voltage amplitude regulation for utility-interconnected fuel cell inverters with an LCL-filter," in *Proc. IEEE Power Electron. Spec. Conf.*, Jun. 2006, pp. 1–6.
[5] T. Hwang, K. Kim, and B. Kwon, "Control strategy of 600 kW E-BOP for molten carbonate fuel cell generation system," in *Proc. Int. Conf. Elect. Mach. Syst.*, Oct. 2008, pp. 2366–2371.
[6] Z. Yao, L. Xiao, and Y. Yan, "Seamless transfer of single-phase grid-interactive inverters between grid-connected and stand-alone modes," *IEEE Trans. Power Electron.*, vol. 25, no. 6, pp. 1597–1603, Jun. 2010.
[7] H. Kim, T. Yu, and S. Choi, "Indirect current control algorithm for utility interactive inverters in distributed generation systems," *IEEE Trans. Power Electron.*, vol. 23, no. 3, pp. 1342–1347, May 2008.
[8] S. Yoon, H. Oh, and S. Choi, "Controller design and implementation of indirect current control based utility-interactive inverter system," in *Proc. IEEE Energy Convers. Congr. Expo.*, Sep. 2011, pp. 955–960.
[9] V. Kaura and V. Blasko, "Operation of a phase locked loop system under distorted utility conditions," *IEEE Trans. Ind. Appl.*, vol. 33, no. 1, pp. 58–63, Jan. 1997.
[10] A. Timbus, R. Teodorescu, F. Blaabjerg, and M. Liserre, "Synchronization methods for three phase distributed power generation systems. an overview and evaluation," in *Proc. IEEE Power Electron. Spec. Conf.*, Jun. 2005, pp. 2474–2481.
[11] F. D. Mango, M. Liserre, A. D. Aquila, and A. Pigazo, "Overview of anti-islanding algorithms for PV systems—Part I: Passive methods," in *Proc. 12th Int. Power Electron. Motion Control Conf.*, Aug. 2006, pp. 1884–1889.
[12] C. E. Rohrs, J. L. Melsa, and D. Schultz, *Linear Control System*. New York: Mcgraw-Hill, 1993.